Electronic Supplementary Material (ESI) for Journal of Materials Chemistry A.
This journal is © The Royal Society of Chemistry 2019

Supporting Information

Gel Electrolytes with Wide Potential Window for High-rate Al-ion Batteries

Zhijing Yu,[a] Shuqiang Jiao,[a, b, *] Jiguo Tu,[a] Wei-Li Song,[b, *] Haiping Lei,[a] Handong Jiao,[b] Haosen Chen[b, *] and Daining Fang[b]

[a] State Key Laboratory of Advanced Metallurgy, University of Science and Technology Beijing, Beijing 100083, P. R. China.

[b] Institute of Advanced Structure Technology, Beijing Institute of Technology, Beijing 100081, P R China.

Corresponding Author

*E-mail addresses: sjiao@ustb.edu.cn (S. Jiao), weilis@bit.edu.cn (W. L. Song), chenhs@bit.edu.cn (H. Chen)

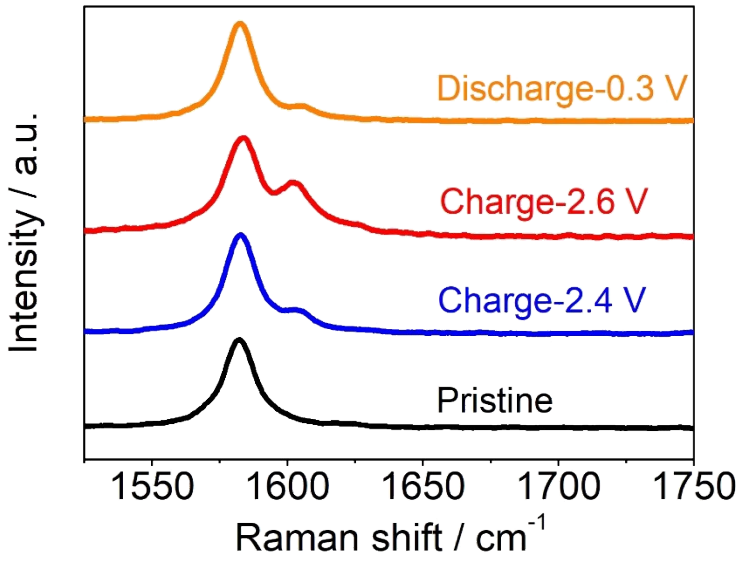

Fig. S1. Raman spectra of the positive electrodes: pristine, charged-2.4 V and charged-2.6 V.

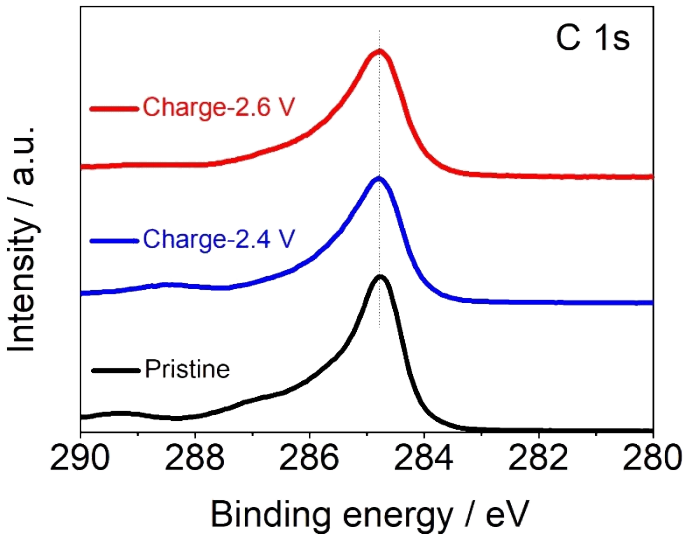

Fig. S2. C 1s peak of the graphitic positive electrodes: pristine, charged-2.4 V and charged-2.6 V.

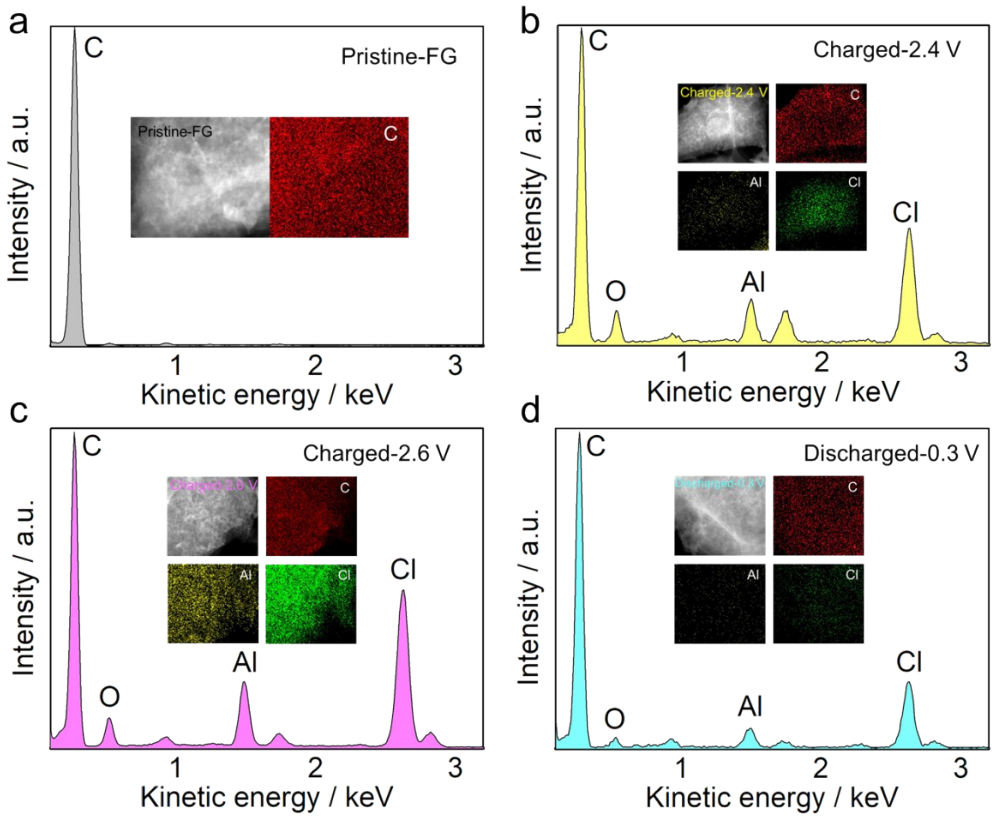

Fig. S3. EDS analysis of the graphitic positive electrodes：(a) Pristine, (b) Charged-2.4 V, (c) Charged-2.6 V and (d) Discharged-0.3 V. The insets are the corresponding EDS mapping images.

Table. S1. EDS element analysis results of the original positive electrode.

Element	Weight (%)	Atom (%)
C K	100.0	100.0

Table. S2. EDS element analysis results of the charged-2.4 V positive electrode.

Element	Weight (%)	Atom (%)
C K	76.75	90.04
Al K	5.76	3.01
Cl K	17.49	6.95

Table. S3. EDS element analysis results of the charged-2.6 V positive electrode.

Element	Weight (%)	Atom (%)
C K	69.58	86.21
Al K	7.72	4.26
Cl K	22.70	9.53

Table. S4. EDS element analysis results of the discharged-0.3 V positive electrode.

Element	Weight (%)	Atom (%)
C K	86.08	94.5
Al K	2.72	1.33
Cl K	11.20	4.17

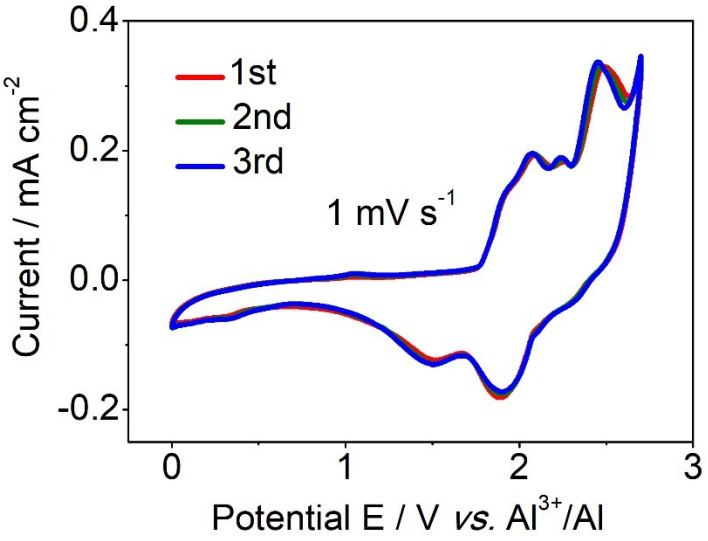

Fig. S4. CV curves of the solid-state AIB at a scan rate of 1 mV s^{-1} in the voltage range of 0–2.70 V.

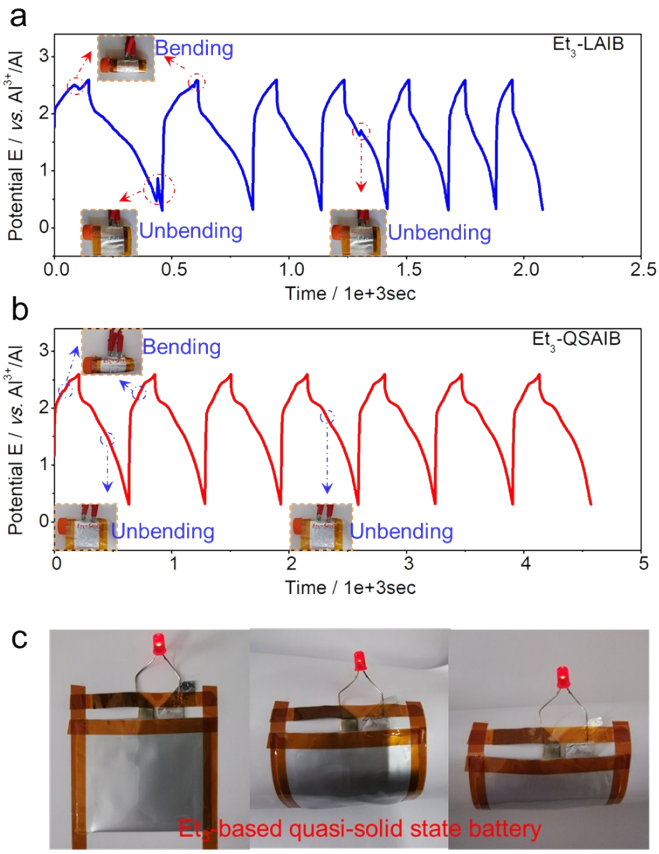

Fig. S5. The charge/discharge curves of the Et_3NHCl-based batteries with different bending states: (a) Liquid system, (b) Quasi-solid system. (c) The AIB with Et_3NHCl-based gel electrolytes operating stably under different bending conditions.

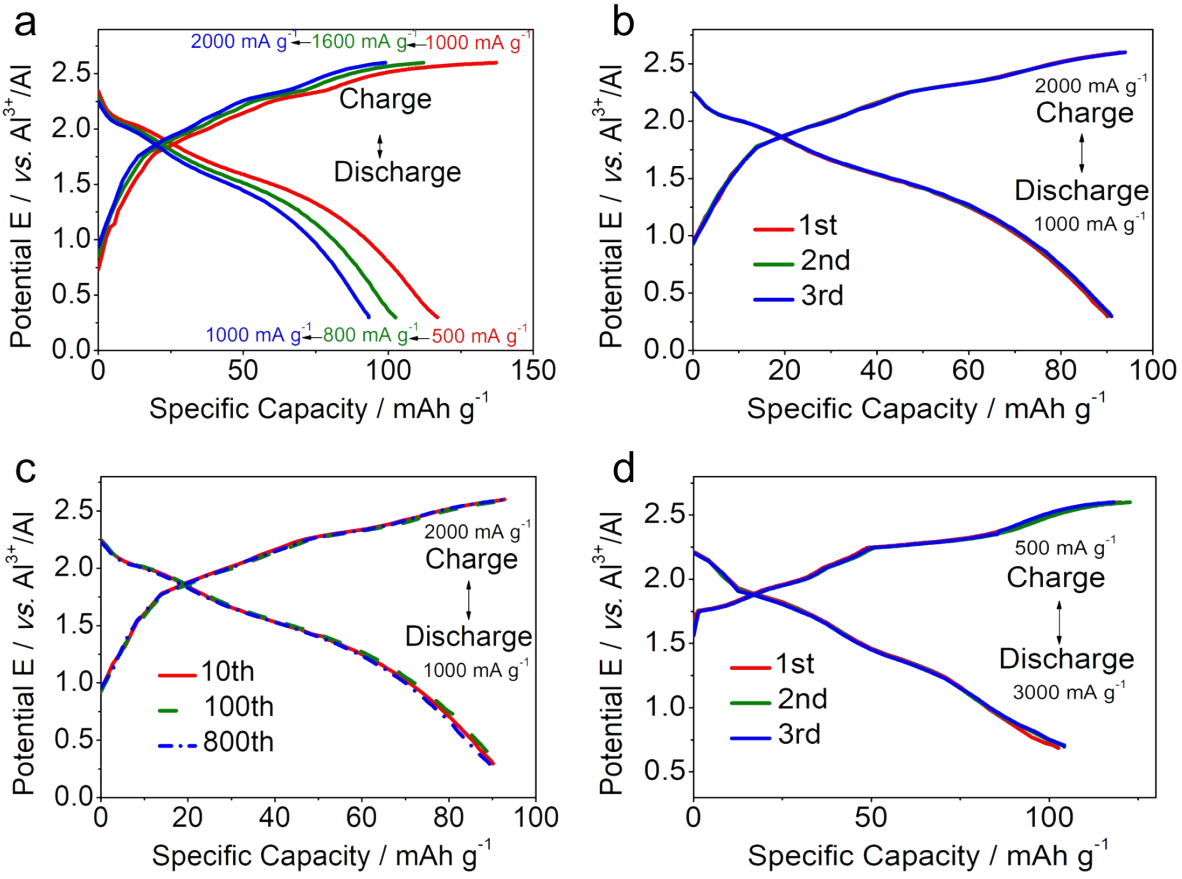

Fig. S6. (a) Galvanostatic charge and discharge profiles of the solid-state batteries at different current densities. (b) The initial three charge and discharge curves. (c) The charge and discharge curves at different cycles. (d) The charge and discharge curves at the charge current density of 500 mA g^{-1} and the discharge current density of 3000 mA g^{-1}.

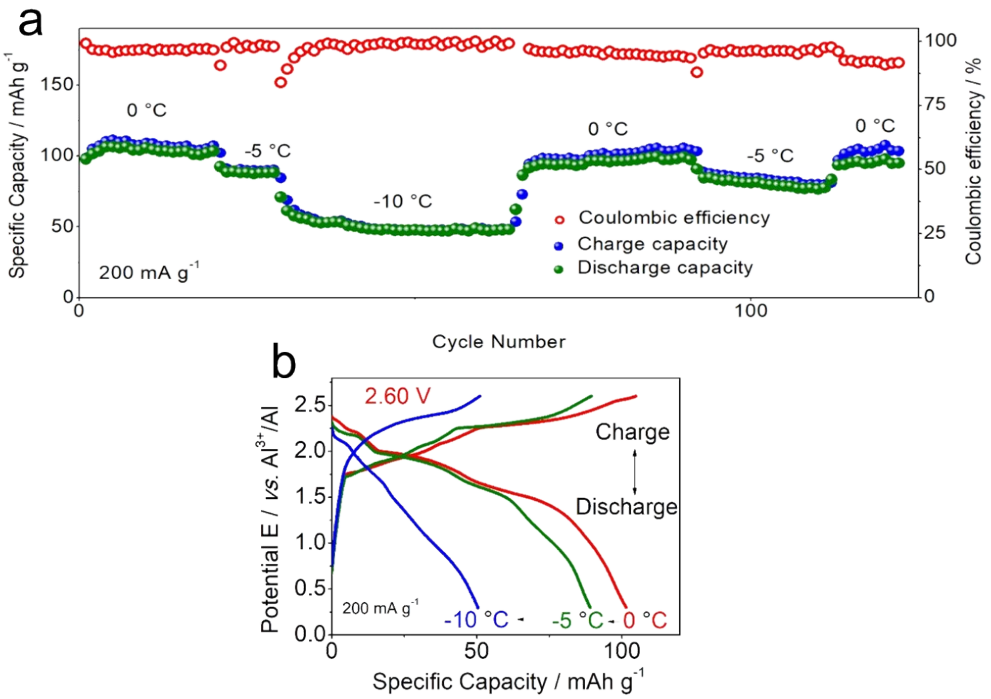

Fig. S7. (a) Cycling stability of the solid-state AIBs at lower temperature (current density of 200 mA g^{-1}). (b) The charge and discharge curves at different temperatures (current density 200 mA g^{-1}).

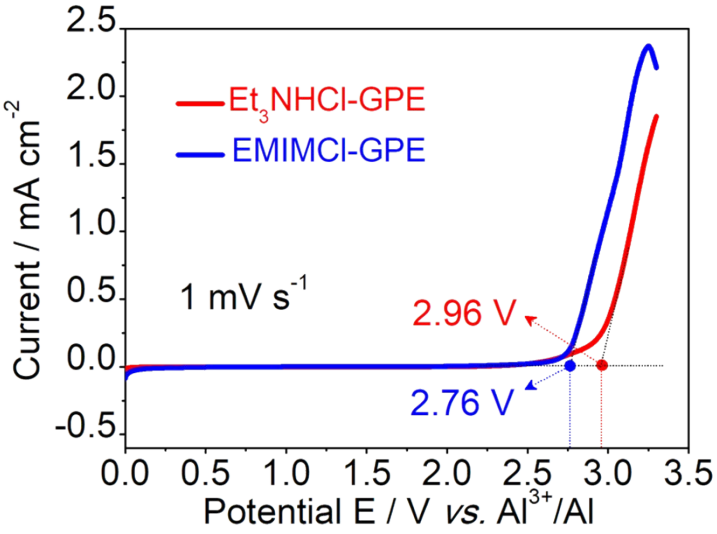

Fig. S8. The comparison of the LSV curves of the two kinds of gel-polymer electrolyte systems.

Table. S5. The values of the ionic conductivities (σ) of Et_3NHCl-based gel-polymer electrolyte with corresponding temperatures

T / ℃	**-20**	**0**	**25**	**40**	**60**	**80**	**100**
σ / S cm^{-1}	2.95×10^{-4}	1.04×10^{-3}	4.52×10^{-3}	7.48×10^{-3}	1.07×10^{-2}	1.47×10^{-2}	1.83×10^{-2}

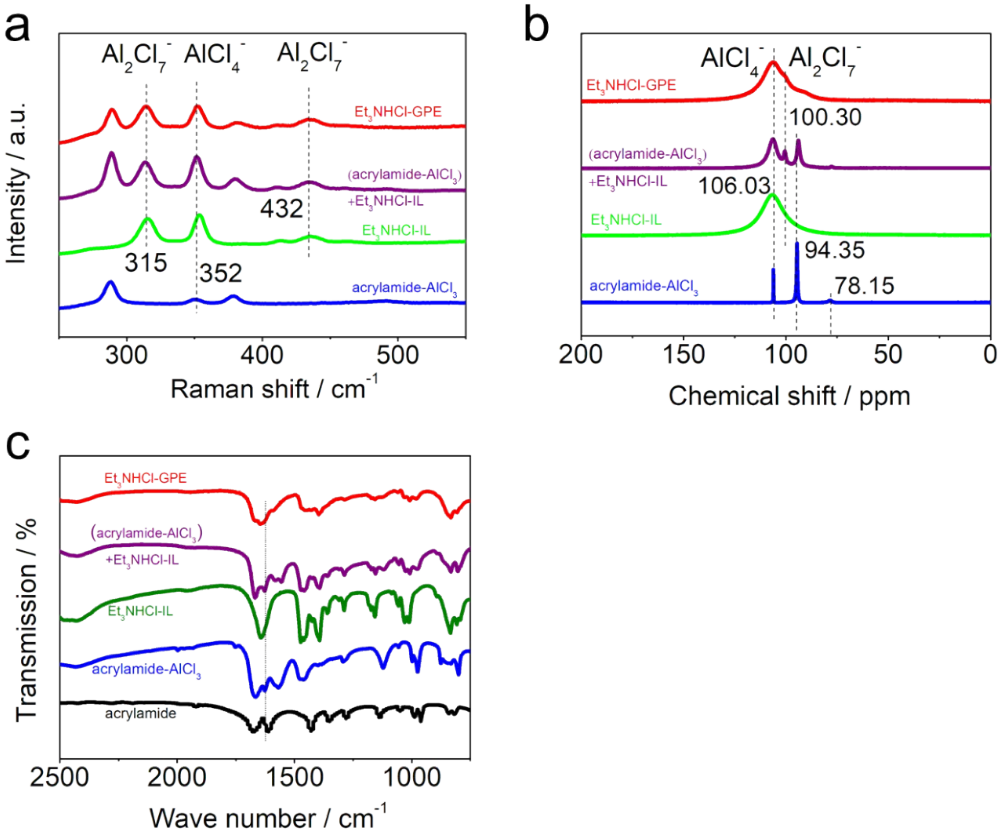

Fig. S9. (a) Raman spectra (b) $_{27}$Al NMR spectra (c) FTIR spectra of the samples during preparation.

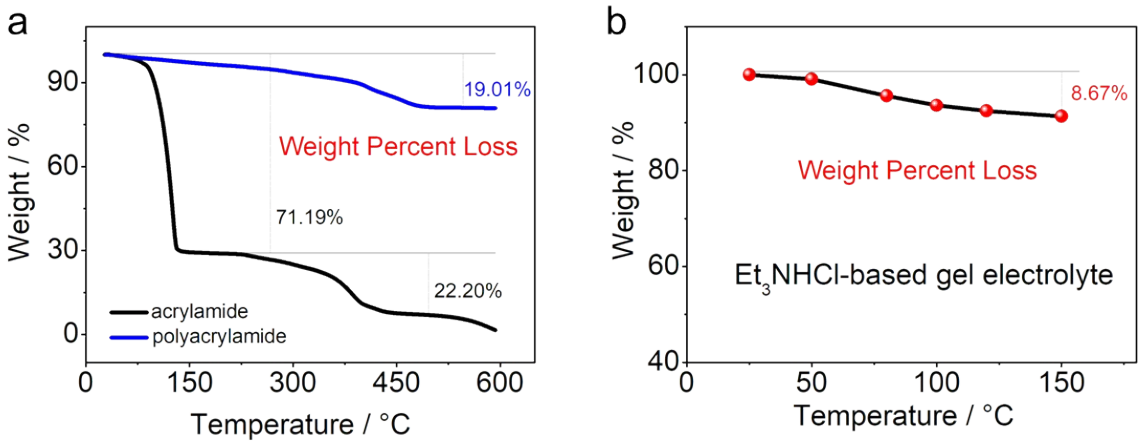

Fig. S10. (a) TG curves of monomer and polymer skeleton of the electrolyte. (b) The mass change during the heating process of the Et_3NHCl-based gel electrolyte.

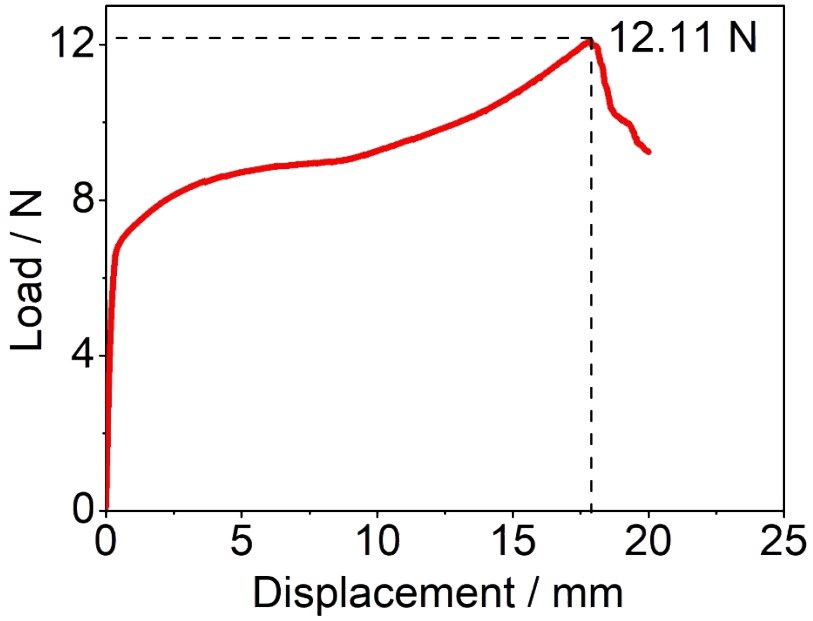

Fig. S11. The load-displacement curve of the Et_3NHCl-based gel electrolyte.

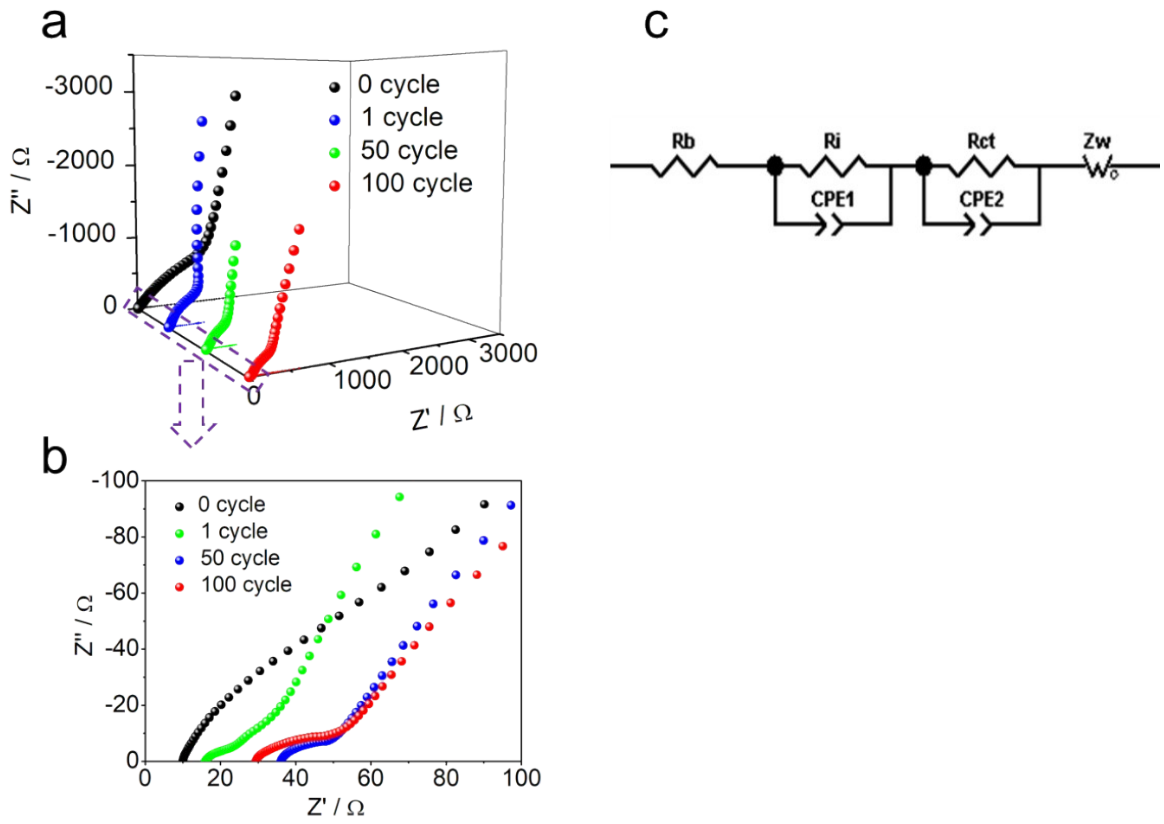

Fig. S12. The electrochemical impedance spectroscopy measurements. (a,b) The Nyquist plots of the solid-state battery after 0, 1, 50 and 100 cycles at a frequency range of 100 kHz to 0.01 Hz with an amplitude of 5 mV. (c) Equivalent circuit model of the studied system.